Si K, Si L, and Cr K x-ray valence-band studies of bonding in chromium silicides: Experiment and theory

A. Šimůnek and M. Polčík
Institute of Physics, Academy of Sciences of the Czech Republic, Cukrovarnická 10, 162 00 Prague 6, Czech Republic

G. Wiech
Sektion Physik der Ludwig-Maximilians-Universität München, Geschwister-Scholl-Platz 1, 80539 München, Federal Republic of Germany

(Received 27 February 1995)

We present Si K, Si L, and Cr K x-ray emission bands of Cr_3Si, CrSi, and $CrSi_2$ together with Si K and Si L emisison bands of Cr_5Si_3. The measured spectra are compared with *ab initio* pseudopotential calculations of the emission bands of Cr_3Si, CrSi, and $CrSi_2$. The Si L spectra were separated into contributions of Si s-like and Si d-like states. Good agreement between theory and experiment is found. The trends in development of spectral features with sample composition can be qualitatively understood by the bonding behavior of Cr and Si atoms.

I. INTRODUCTION

Stimulated by their potential applicability in microelectronic devices, the electronic structure of chromium silicides has been the subject of intensive experimental and theoretical investigations and the underlying principles of the chemical bonding were thoroughly discussed in Refs. 1–4. The purpose of this paper is (i) to present measured and calculated Si K, Si L, and Cr K x-ray valence-band spectra of a series of chromium silicides—Cr_3Si, Cr_5Si_3, CrSi, and $CrSi_2$—in which the ratio of chromium to silicon atoms varies in a wide range and (ii) to relate the shapes of the spectra to changes in bonding. Since the nearest-neighbor atoms and also the local geometry in these crystals are quite different we expect different bonding behavior of these silicides. In the first compound of the series, Cr_3Si, there are bonding distances between Cr-Cr and Cr-Si atoms, but not between Si-Si atoms. In Cr_5Si_3 and CrSi there are Cr-Cr, Cr-Si, and Si-Si bonding distances, while in $CrSi_2$ no Cr-Cr bonding distances exist.

X-ray emission spectroscopy provides very detailed information about the valence electron states of a compound or alloy because of its site and symmetry selectivity. The measured Si K, Si L, and Cr K emission bands of the chromium silicides presented in this paper reflect the behavior of the silicon p- and s-like valence electrons and the creation of silicon d- and chromium p-like electron states by the bonds (note, Si d and Cr p states are not occupied in free atoms). The analysis of the experimental results is based on *ab initio* calculations of the electronic structure and of x-ray emission bands. We applied the pseudopotential method using a plane-wave basis that imposes no shape approximations on either the charge density or the potential. We will show that these calculations in most cases provide spectra that are in excellent agreement with the experimental results. The contributions of Si s- and Si d-like states to Si L bands have been calculated separately and it becomes evident how important Si d-like states are for the interpretation of Si L emission bands. Finally it will be shown that the significant discrepancies noted by Weijs *et al.*[5] between partial density of states (DOS) and measured Si K and Si L bands do not necessarily have to be attributed to self-energy effects.

The paper is organized as follows. In Sec. II experimental and in Sec. III computational details are given. In Sec. IV the experimental and theoretical results are presented, and they are discussed in Sec. V. All results are briefly summarized in Sec. VI.

II. EXPERIMENT

For the measurement of the Si K, Si L, and Cr K emission bands three different spectrometers were used. The samples were prepared by crushing the very hard pieces of the silicides with a steel pestle and mortar, and then rubbing the powder on a substrate of copper (Si K, 24×25 mm^2; Si L) or pressing it on an aluminum holder (Cr K, 30×14 mm^2). For $CrSi_2$ we observed some differences between the calculated and measured Si L emission bands. Therefore we checked the homogeneity of the crystal phase and contamination by impurity atoms. The x-ray diffraction test with the DRON2 powder diffractometer showed that the $CrSi_2$ sample consists of a single hexagonal phase. According to the electron beam excited microanalysis using the JEOL Superprobe 733 electron microscope, $CrSi_2$ contains less than 3 at. % impurity atoms.

A. Si K emission bands

The Si K emission bands were measured with a high-vacuum Johann-type spectrometer (pressure $\sim5\times10^{-6}$ hPa). The x-ray tube was operated at 5.98 kV and about 180 mA. The x-ray radiation of a tungsten anode was

used for the excitation of the samples (fluorescence excitation). The comparatively low voltage was applied to avoid excitation of chromium K radiation and to reduce the background. The dispersing element was a quartz crystal ($50\times25\times0.3$ mm^3) cut parallel to the $10\bar{1}0$ plane and bent to a radius of 109 cm. The detector was a position-sensitive proportional counter with a backgammon cathode.[6] The acquisition time for 8000–10 000 counts at the peak position of the spectra varied from about 100 to 180 h depending on the silicon content of the samples and the peak/background ratio was about 2.7. The energy resolution of the spectra was about 0.7 eV.

B. Si L emission bands

The Si L emission bands were measured with a 2-m grazing incidence concave grating spectrometer using electron bombardment (3.0 kV, 1.0 mA, size of focal spot $\sim3\times9$ mm^2; pressure $\sim2\times10^{-8}$ hPa). The grating was gold coated with 600 lines/mm and a blaze angle of 1°31′. The detector was a parallel-plate photoelectron multiplier.[7] The spectra were measured repeatedly in the step-scanning mode. The total measuring time for the Si L emission bands varied from 50 h for $CrSi_2$ to about 100 h for Cr_3Si. The corresponding peak/background ratios varied from 13:1 to 4:1. The energy resolution of the spectrometer was ~0.7 eV at a photon energy of 95 eV.

C. Cr K emission bands

The Cr K emission bands were measured using a two-crystal spectrometer[8] and fluorescence excitation. The analyzing crystals were Si(220) and Ge(111) in the (m,n) position. The width of the spectral window, which gives the resolution of the spectrometer, can be calculated; it resulted in 0.8 eV. The measurements were performed in the step-scanning mode. Each measured point of the Cr K emission bands represents the average of repeated measurements. The statistical error of each point is less than 3%, the intensity was monitored by the Cr $K\beta_{1,3}$ core line ($M_{2,3}\rightarrow K$). For the calibration of the photon energy the Cr $K\beta_{1,3}$ core line of Cr_2O_3 was used. A linear background was subtracted from the measured spectra. This procedure is not fully correct because near the valence-band maximum the shape of the background can change due to self-absorption and anomalous dispersion of the primary radiation in the sample. However, there was no substantial change of the shapes of all emission bands after subtracting the background, which indicates that no artificial structures were created.

III. COMPUTATIONS

The standard *ab initio* pseudopotential method was used to calculate the single-particle energy levels within the local density approximation (LDA). Exchange and correlation effects were included via the Hedin and Lundqvist formula.[9]

The Si and Cr pseudopotentials were generated by the phase-shift technique proposed by Vackář and Šimůnek.[10] In the case of Cr, we used the configuration [Ar] $3d^{3.5}$, $4s^2$, $4p^{0.5}$ to generate the s, p, and d semilocal potentials. These potentials were used for all calculations of the electronic structure and the x-ray emission bands presented in this paper. The potential permitted a tractable computation with a cutoff in kinetic energy of 36 Ry. The calculations for metallic chromium and the chromium silicides were carried out using the real crystal structures, i.e., Cr bcc, Cr_3Si A15, CrSi B20, and $CrSi_2$ C40.[11] No calculations were performed for Cr_5Si_3 because of the size of the unit cell that contains 32 atoms.

For the calculation of the x-ray transition matrix elements the core functions $\Psi_c^l(\mathbf{r})$ and the valence functions $\Psi_v(\mathbf{r},\mathbf{k})$ are written in the following form:

$$\Psi_c^l(\mathbf{r})=R_l(r)Y_{lm}(\mathbf{r})$$

and

$$\Psi_v(\mathbf{r},\mathbf{k})=\sum_G a_G(\mathbf{k})e^{i(\mathbf{k}+\mathbf{G})\cdot\mathbf{r}}\ ,$$

where l is the angular momentum of the core state, $\mathbf{G}$ are reciprocal vectors, and the $a_G(\mathbf{k})$ are eigenvectors of the Hamiltonian. Using the expression

$$e^{i\mathbf{k}\cdot\mathbf{r}}=4\pi\sum_{l=0}^{\infty}i^l j_l(kr)\sum_{m=-l}^{+l}Y_{lm}(\mathbf{r})Y^*(\mathbf{k})\ ,$$

the dipole transition matrix element splits in its radial and angular parts

$$\langle\Psi_c^l(\mathbf{r})|\mathbf{e}\cdot\mathbf{r}|\Psi_v(\mathbf{r},\mathbf{k})\rangle=4\pi\sum_G a_G(\mathbf{k})\sum_{l'=0}^{\infty}i^{l'}\langle R_l|r|j_{l'}(|\mathbf{k}+\mathbf{G}|)\rangle_{\text{rad}}\times\sum_{m=-l'}^{l'}\left\langle Y_{lm}\left|\frac{\mathbf{e}\cdot\mathbf{r}}{r}\right|Y_{l'm'}\right\rangle_{\text{ang}}Y^*_{l'm'}(\mathbf{k}+\mathbf{G})\ ,$$

where $\mathbf{e}$ is the polarization vector.

In the matrix element the angular momenta are $l=0$ and $l=1$ for the K and L emission bands, respectively; for the valence states of the K and L emission bands the dipole selection rules yield the momenta $l'=1$ and $l'=0$ or 2, respectively. Since the spherical harmonics $Y^*_{l'm'}(\mathbf{k}+\mathbf{G})$ can be expressed by the components of $\mathbf{k}+\mathbf{G}$, the angular part of the transition matrix element was calculated using the plane-wave basis set mentioned above. On the other hand, in the radial part $\langle R_l|r|j_{l'}\rangle_{\text{rad}}$ the Bessel functions j_l describe nodeless behavior of pseudo valence wave functions Ψ_v in the core region of atoms and therefore this radial term cannot be used for calculations of the x-ray transitions. In fact the radial part of

the matrix element is given by integration only in the close vicinity of the atomic nucleus since the radial functions R_l of the core states Cr 1*s*, Si 1*s*, and Si 2*p* are well localized in the cores of atoms. In view of the frozen core approximation forming the basis of the pseudopotential approach the wave functions of valence electrons have a frozen atomic character in the core region, i.e., behavior of the valence wave functions in the core region is nearly atomiclike. Therefore the radial part of the matrix element can be approximated by using atomic wave functions.

In this work we used atomic wave functions for calculations of the radial part of the matrix element taking into account the new *s-p-d* electron configuration of the valence electrons of atoms created by the Cr-Si bond. The nodal structure of silicon valence wave functions was studied earlier for several configurations and ionicities of the silicon atom in crystal and also compared with the nodal structure calculated directly from pseudopotential quantities.[12] It was found that the results of the various approximations for the radial part of the matrix elements in the case of silicon differ less than 10%.

In the case of chromium the core region of the Cr 1*s* state is even smaller than in silicon, and therefore the nodal structure of the valence functions in the core region of the atoms in the crystal is practically identical with that in the free atom.

In order to compare the theoretical results with the measured spectra, the calculated spectra were convoluted with a Lorentzian whose FWHM $w(E)$ varies according to

$$w(E)=w_c+(E/w_b)^2 w_h \ ,$$

where E is the energy measured from the top of the valence band, the width of which is w_b; w_c is the natural width of the core level.[13] The parameter w_h takes into account the lifetime of holes in the valence band. For w_h the value 1 eV was used. In addition, all calculated spectra were convoluted with a 0.5-eV FWHM Gaussian to take into consideration instrumental effects.

The computational techniques described above were used for the calculations of the Si *K* and Si *L* emission bands of silicon and the Cr *K* emission band of chromium. In Fig. 1 the results of the *ab initio* calculations are compared with the measured spectra. There is very good agreement between theory and experiment indicating the plausibility of the approximations used.

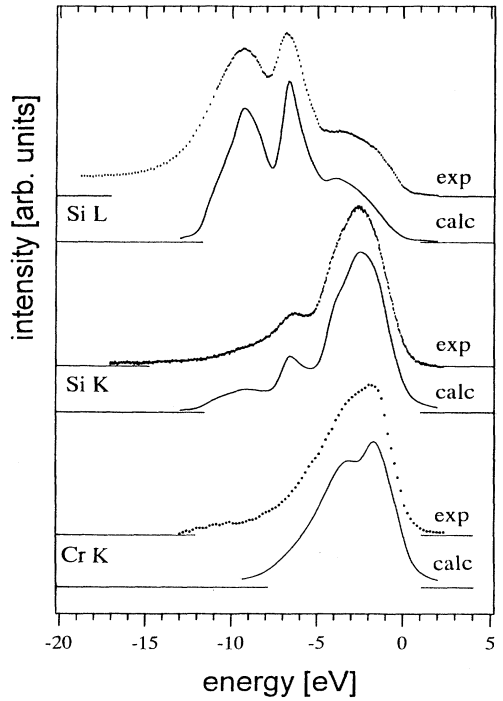

FIG. 1. Measured and calculated Si *L* and Si *K* emission bands of silicon and Cr *K* emission band of metallic chromium on a common binding energy scale.

IV. EXPERIMENTAL RESULTS

In Figs. 2, 3, and 4 the experimental results of the Si *K*, Si *L*, and Cr *K* emission bands are presented, respectively. The intensity of all emission bands is normalized to the same height. In the following the spectra and their main characteristics will be described briefly. The positions of the maxima of the emission bands are listed in Table I.

A. Si *K* emission bands

The Si *K* emission band of Cr_3Si (Fig. 2) is comparatively narrow with a sharp peak. At about 1832 eV the intensity changes abruptly: the rapid decrease of intensity is followed by a gentle decrease towards lower photon energy. On the high-energy side there is also a bend in intensity drop at about 1837 eV, leading to a clearly visible shoulder (from 1837 to 1839 eV).

With increasing silicon content, i.e., in going from Cr_3Si over Cr_5Si_3 to CrSi the abrupt change of intensity at 1832 eV is maintained as well as the sharp peak. Its maximum is slightly shifted towards higher photon energy (Table I) and also the width (FWHM) of the spectra increases towards higher energy. This gradual development does not continue to $CrSi_2$ (Fig. 1). In the Si *K* emission band of $CrSi_2$ only the abrupt change of intensity ($\sim$1832 eV) is maintained; the intensity at lower energy, however, is higher than in the other spectra. The width of the band has further increased. The position of the maxima is shifted to higher photon energy, thus lead-

TABLE I. Photon energies of the main maxima of Si *K*, Si *L*, and Cr *K* emission (eV).

Material	Si *K*	Si *L*	Cr *K*
Cr			6535.2
Cr_3Si	1835.3	89.7	6534.3
Cr_5Si_3	1835.5	89.9	
CrSi	1835.7	90.3	6534.0
$CrSi_2$	1837.2	91.5	6533.9
Si	1835.9	91.9	

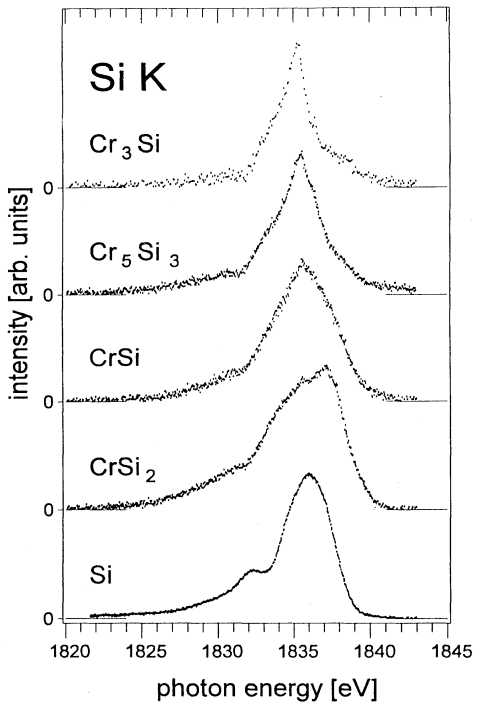

FIG. 2. Si K emission bands of Cr_3Si, Cr_5Si_3, CrSi, $CrSi_2$, and Si; original measurements with a linear background subtracted; photon energy scale.

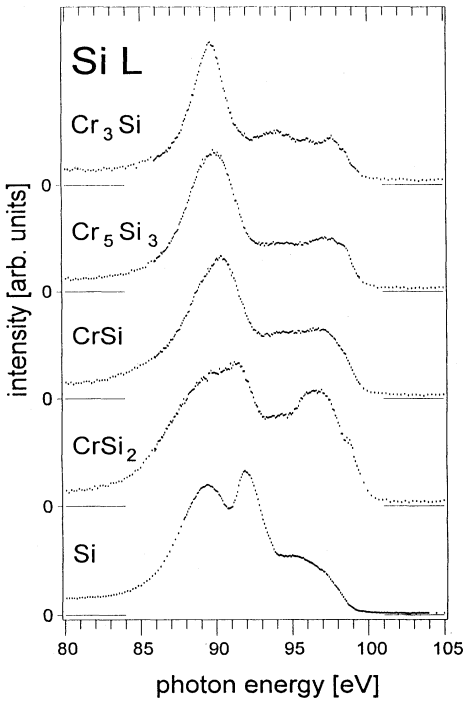

FIG. 3. Si L emission bands of Cr_3Si, Cr_5Si_3, CrSi, $CrSi_2$, and Si; original measurements with a linear background subtracted; photon energy scale.

ing to a steeper high-energy edge of the spectrum. Moreover the maximum is followed by a shoulder on the low-energy side at 1835 eV.

At the bottom of Fig. 2 the Si K emission band of pure silicon is shown for comparison.

B. Si L emission bands

The Si L emission bands of Cr_3Si, Cr_5Si_3, and CrSi (Fig. 2) are similar in shape. All spectra exhibit a pronounced peak and a plateau towards higher photon energy. With increasing silicon content this peak becomes broader, the maximum is shifted to higher photon energy (Table I), and the intensity of the plateau increases. In all spectra the plateau contains some features.

Going from CrSi to $CrSi_2$ the shape of the spectrum changes significantly. The main peak has become even broader and split in two features. Compared to CrSi the maximum is shifted by ~ 1.2 eV to higher photon energy. Within the area of the plateau a broad peak (~ 96.5 eV) has developed, and a small shoulder at about 98.5 eV. On the whole the intensity between 93 and ~ 98 eV is considerably higher than for the spectra of CrSi, Cr_5Si_3, and Cr_3Si. At the bottom of Fig. 3 the Si L emission band of silicon is shown for comparison. It has two distinct peaks at 89.4 and 92.0 eV. The plateau at 95 eV is very short followed by a gradual decrease in intensity towards higher energy.

C. Cr K emission bands

Compared to the Cr K emission band of metallic chromium the maxima of Cr_3Si, CrSi, and $CrSi_2$ (Fig. 4) are shifted to lower photon energy by 0.90, 1.20, and 1.30 eV, respectively (Table I), and in addition the spectra of the silicides extend to lower photon energy. Particularly Cr_3Si and CrSi form a broad shoulder below -4 eV. The Cr K band of metallic chromium has a FWHM of only 4.85 eV. The largest FWHM is for Cr_3Si (5.75 eV) and it decreases with decreasing Cr content in the samples (CrSi: 5.55 eV; $CrSi_2$: 5.45 eV). We had not enough material to measure also the Cr K emission band of Cr_5Si_3; the measurements using a two-crystal spectrometer require more material for sample preparation than using the other two spectrometers mentioned.

The Cr K emission band of $CrSi_2$ differs from the other spectra in that it has a narrow peak and shows a clearly visible shoulder at ~ 6532 eV. The intensity of the "tail" below ~ 6530 eV is comparable to that of CrSi and higher than in Cr_3Si.

V. DISCUSSION

To understand the similarity of the shapes of the emission bands of Cr_3Si, Cr_5Si_3, and CrSi we should realize that in all these crystals there are Cr-Cr bonding distances contrary to $CrSi_2$. In Cr_3Si and Cr_5Si_3 the shortest distances between Cr atoms are 2.28 and 2.32 Å, respec-

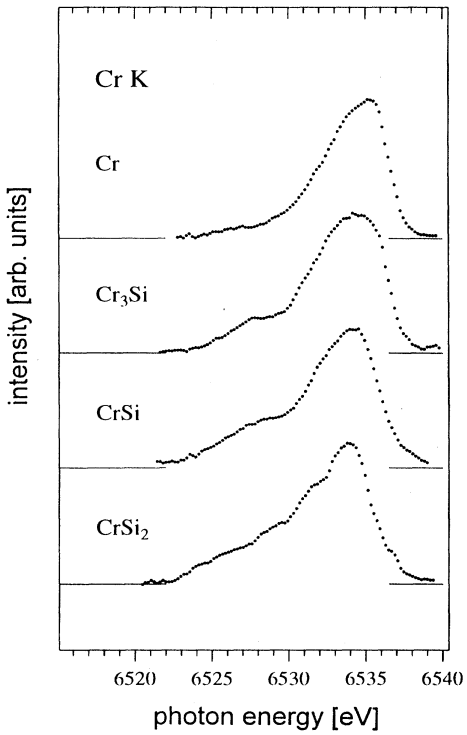

FIG. 4. Cr K emission bands of metallic Cr, Cr_3Si, CrSi, and $CrSi_2$; original measurements with a linear background subtracted; photon energy scale.

tively. These distances are even shorter than in metallic chromium (2.49 Å). In Cr_3Si the bonding distance between Cr and Si atoms is 2.55 Å. Cr_5Si_3 has a much more complicated structure and the Cr-Si distances range from 2.43 to 2.66 Å. The various strengths of Cr-Si bonds and the additional contribution of Si-Si bonds broaden the spectral features of all emission bands of Cr_5Si_3 compared to those of Cr_3Si (Figs. 2–4).

In the case of CrSi the Cr-Si distances range between 2.32 and 2.58 Å, 2.32 Å being the shortest Cr-Si distance of all samples studied here. The Cr-Cr and Cr-Si distances are quite large: 2.83 and 2.85 Å, respectively. As a consequence of the various strengths of the Cr-Si bonds in CrSi we observe further broadening of the Si K emission band (Fig. 2) and a nearly structureless plateau in the Si L emission band (Fig. 3). On the other hand, the main peak of the Cr K emission band of CrSi is narrower than those of Cr_3Si and Cr_5Si_3 (Fig. 4), thus reflecting the larger distance between the Cr atoms (2.83 Å).

As already mentioned in Sec. IV the similarity and the gradual development of spectral features observable in the emission bands of Cr_3Si, Cr_5Si_3, and CrSi does not continue to $CrSi_2$. The main reason for this is that the Cr-Cr distance (3.06 Å) is quite large and therefore does not play a significant role in bonding, while the Cr-Si and Si-Si bonds (bond lengths 2.47 and 2.55 Å for both bonds) are decisive for the electronic structure of $CrSi_2$. The virtual absence of Cr-Cr bonds and the dominance of Cr-Si and Si-Si bonds lead to two effects observable in the spectra.

First, the Cr-Cr bonds create core-level shifts that differ from those core-level shifts induced by Cr-Si bonds. We have measured the Cr $K\beta_{1,3}$ line corresponding to the core-level transition $Cr3p \rightarrow Cr1s$, and we have found that the energies E of the Cr $K\beta_{1,3}$ line are related by $E(\text{Cr met}) - 0.1\ \text{eV} = E(Cr_3Si) = E(CrSi) = E(CrSi_2) + 0.25$ eV, i.e., the highest photon energy corresponds to metallic chromium, the lowest to $CrSi_2$.

Second, the nearest neighbors of Cr atoms in $CrSi_2$ are only Si atoms, there are no Cr-Cr bonds as in the other compounds. As a consequence the Cr atoms induce more silicon d-like states on Si atoms than in the other silicides, and this effect increases intensity of the Si L emission band of $CrSi_2$ at the top of the valence band.

After this more general discussion based on interatomic distances and bond strengths we will discuss the single compounds in more detail and compare measured spectra with calculated emission bands. In Figs. 5–7 we present the Si L, Si K, and Cr K emission bands of Cr_3Si, CrSi, and $CrSi_2$ on a common energy scale. In each figure the dashed line in the calculated Si L band indicates the contribution of Si d states to the spectrum. Additionally, at the bottom of the figures the total density of states (TDOS) is presented.

A. Cr_3Si

In Fig. 5 are shown the measured and calculated Si L, Si K, and Cr K emission bands of Cr_3Si together with the

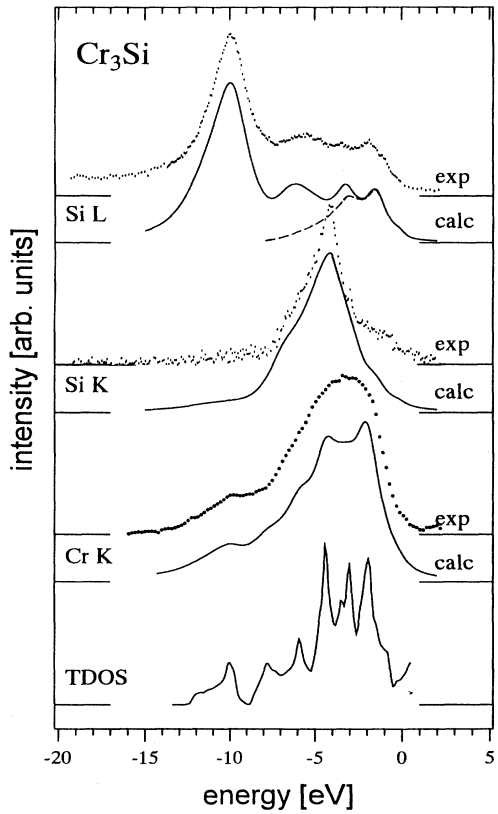

FIG. 5. Measured and calculated Si L, Si K, and Cr K emission bands and TDOS of Cr_3Si; the dashed curve in the Si L spectrum represents the contribution of Si d-like electrons.

total density of states. The upper part of the valence states arises from the bonding combinations of Si p and Cr d electrons and additionally created Si d and Cr p states observable in the Si L and Cr K emission bands, respectively. The lower part of the valence band is derived from Si s electrons; their hybrids create a small amount of Cr p-like states reflected at about -10 eV in the Cr K emission band. All spectral features of the experimental results are reproduced by the calculations, and there is also very good quantitative agreement between theory and experiment.

The electronic structure of Cr_3Si was studied earlier by Franciosi *et al.*[3] applying self-consistent augmented-spherical-wave calculations to Cr_3Si with Cu_3Au structure (which is simpler than the real Cr_3Si structure), and also by Franciosi *et al.*[4] who applied semiempirical extended-Hückel-theory calculation to the actual Cr_3Si structure. Both calculations exhibit a narrow inner valence band at -8 eV (width ~ 1 eV), which is also present in our calculation (~ -9 eV). The agreement between the upper part of our TDOS curve (-7 eV to $E_F=0$; Fig. 5) and the results of Ref. 3 is good, contrary to the TDOS curve of Ref. 4.

B. CrSi

Figure 6 shows the measured and calculated Si L, Si K, and Cr K emission bands and the TDOS of CrSi. All

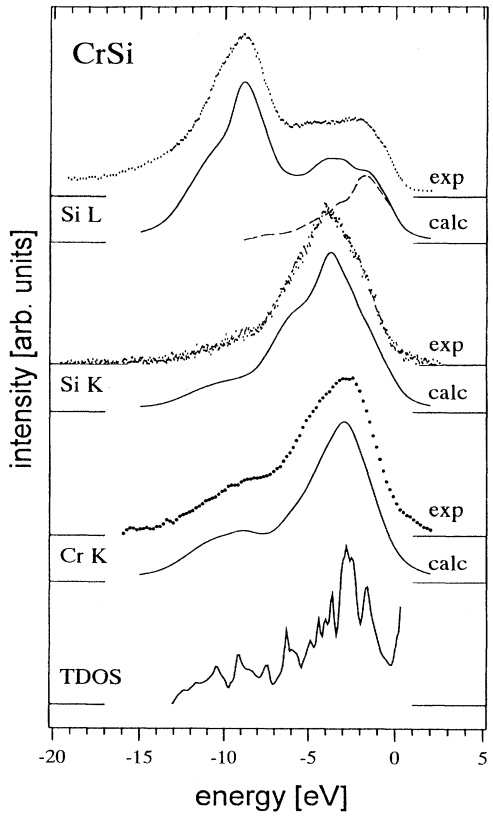

FIG. 6. Measured and calculated Si L, Si K, and Cr K emission bands and TDOS of CrSi; the dashed curve in the Si L spectrum represents the contribution of Si d-like electrons.

significant features in the measured spectra are well reproduced by the calculations in the case of the Cr K and Si K emission bands. There is also good quantitative agreement between the measured and calculated Si L band, except for the higher intensity between -3 and -4 eV in the calculated spectrum.

Si d-like states play an essential role in the upper part of the Si L band. The lack of Si d states in the calculations of Weijs *et al.*[5] yields an incorrect intensity in the corresponding energy range of their results. The lowest Si s states at -11 eV form a weak shoulder in the Si L emission band (Fig. 6, top curves) while in the calculations of Weijs *et al.*[5] they form a pronounced peak and also increase the total width of the band, in disagreement with our calculations and experiment.

The electronic structure of CrSi was already studied by Franciosi *et al.*[3] who used the more simple CuAu structure and by Franciosi *et al.*[4] according to real structure applying the computational techniques mentioned above. The results of Ref. 3 do not show an inner valence-band gap in accordance with our results (Fig. 6), contrary to the results of Ref. 4 (gap at ~ 7–8 eV). On the other hand, in the upper part of the valence band (-7 eV to E_F) our TDOS curve is in better agreement with that of Ref. 4 than of Ref. 3.

C. $CrSi_2$

In Fig. 7 we present the Si L, Si K, and Cr K emission bands of $CrSi_2$ together with the TDOS. On the whole there is good accordance of calculations with experiment, except for the intensities at about -12 eV in the calculated Si L and Cr K emission bands that are too high. With respect to the shape of emission bands we should keep in mind that the Auger process, where a core hole or a hole in the valence band relaxes by emitting an electron, is competing with the x-ray process. Auger processes limit the lifetime of core or valence-band vacancies and by that contribute to a broadening of the observed spectrum. We included these effects phenomenologically using an energy-dependent Lorentzian broadening (see end of Sec. III). The empirical parameter $w_h=1$ eV was applied to all spectra presented in Fig. 1 and Figs. 5–7. In fact the parameter w_h cannot have the same value for all compounds studied in this work: its value depends on the valence wave functions and their overlap. Therefore w_h should be smaller for the more localized Si s-like states in Cr_3Si than for the Si s-like states in silicon or $CrSi_2$. Indeed we have found that the use of greater values of w_h improves the agreement with experiment in the case of silicon (Fig. 1): shallower valley at -7.5 eV and more rounded peak at 9.5 eV in the Si L band and a smoother tail (-8 to -12 eV) in the Si K band. An analogous improvement of agreement between experiment and calculation is also obtained for the Si L, Si K, and Cr K emission bands of $CrSi_2$ by using greater values of w_h (2–4 eV) for the Lorentzian broadening.

The electronic structure calculations performed in the actual $CrSi_2$ structure were presented in Refs. 4, 5, and 14. Our pseudopotential and Mattheiss'[15] linear augmented plane wave one-electron band structure yield

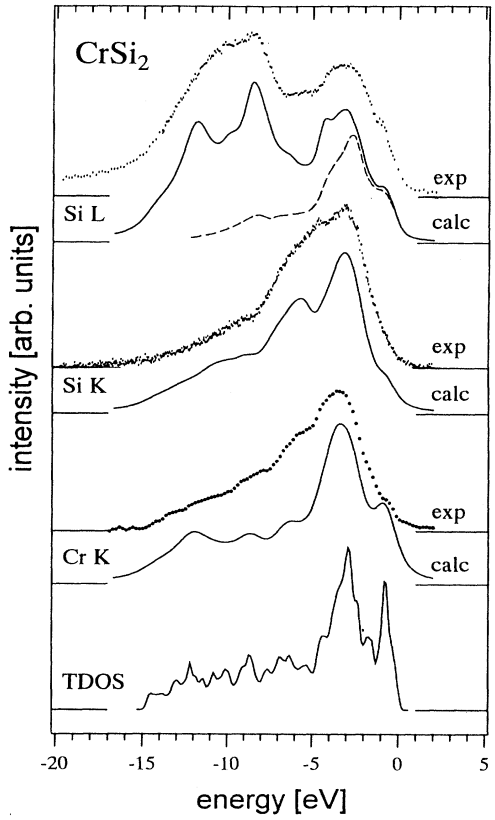

FIG. 7. Measured and calculated Si L, Si K, and Cr K emission bands and TDOS of $CrSi_2$; the dashed curve in the Si L spectrum represents the contribution of Si d-like electrons.

nearly identical TDOS and a total width of the valence band in agreement with experiment. The valence band calculated by Weijs *et al.*[5] is broader and there is a considerable difference between the convoluted sum of silicon s and d partial densities of states and the measured Si L band. Moreover silicon p partial density of states is broader than the observed Si K band.

The differences between the x-ray bands and the corresponding partial densities of states were explained by Weijs *et al.*[5] in terms of self-energy effects. With respect to our results we do not think that self-energy effects play an essential role in x-ray emission bands of chromium silicides. We believe that the differences between the experiment and the calculated DOS in Ref. 5 arise from an incorrect summation of Si s and Si d contributions (the same weight in Ref. 5) and inaccurate shapes of the partial DOS caused by the augmented spherical-wave technique applied.

VI. SUMMARY

In this paper we presented measurements of Si K, Si L, and Cr K emission bands of Cr_3Si, CrSi, and $CrSi_2$ together with *ab initio* calculations of the electronic structure and the emission bands of these compounds. In addition the Si K and Si L emission bands of Cr_5Si_3 were measured. All features in the spectra can be attributed to Si s, Si p, Si d, and Cr p derived states. The K emission bands reflect Si p and Cr p derived states. Because for the Si L emission bands both the Si s and Si d contributions were calculated, it became evident that Si d states play an important role for the interpretation of the Si L spectra. Comparison of experimental with theoretical results shows that *ab initio* LDA calculations describe the electron states and the x-ray emission bands of the chromium silicides under study in good agreement with measured spectra.

ACKNOWLEDGMENTS

We would like to thank S. Reiter and J. Biermann for their help in acquiring the Si L and Si K emission bands, respectively. This work was supported by project No. X 242.22 of Bilaterale Zusammenarbeit mit der Tschechischen Republik and the projects 202/93/1164 and 202/93/0154 of the Grant Agency of the Czech Republic. The use of the CRAY Y-MP EL in Prague was partially sponsored by Westinghouse Electric. A.Š. is greatly indebted to Leibniz-Rechenzentrum der Bayrischen Akademie der Wissenschaft, München, for generously making available computer facilities.

[1] J. H. Weaver, A. Franciosi, and V. L. Moruzzi, Phys. Rev. B **29**, 3293 (1994).
[2] W. Speier, E. v. Leuken, J. C. Fuggle, D. D. Sarma, L. Kumar, B. Dauth, and K. H. J. Buschow, Phys. Rev. B **39**, 6008 (1989).
[3] A. Franciosi, D. J. Peterman, J. H. Weaver, and V. L. Moruzzi, Phys. Rev. B **25**, 4981 (1982).
[4] A. Franciosi, J. H. Weaver, D. G. O'Neill, F. A. Schmidt, O. Bisi, and C. Calandra, Phys. Rev. B **28**, 7000 (1983).
[5] P. J. Weijs, H. van Leuken, R. A. de Groot, J. C. Fuggle, S. Reiter, G. Wiech, and K. H. J. Buschow, Phys. Rev. B **44**, 8195 (1991).
[6] W. Zahorowski, J. Mitternacht, and G. Wiech, Measurement Sci. Technol. **2**, 602 (1991).
[7] W. Schnell and G. Wiech, Mikrochim. Acta Suppl. **7**, 323 (1977).
[8] J. Drahokoupil and A. Fingerland, in *Advances in X-Ray Spectroscopy*, edited by C. Bonnelle and C. Mande (Pergamon, 1982), p. 167.
[9] L. Hedin and B. I. Lundqivst, J. Phys. C **4**, 2064 (1971).
[10] J. Vackář and A. Šimůnek, Solid State Commun. **81**, 837 (1992).
[11] G. Bergerhoff, R. Hundt, R. Sievers, and D. I. Brown, J. Chem. Inform. Comput. Sci. **23**, 66 (1983); CRYSTIN—Crystal Structure Information System, produced by Fachinformationszentrum (FIZ) Karlsruhe and Gmelin-Institut für Anorganische Chemie der Universität Bonn. Release January 1994.
[12] J. Vackář and A. Šimůnek, J. Phys. Condens. Matter **6**, 3025 (1994), **5**, 867 (1993).
[13] D. A. Goodings and R. Harris, J. Phys. C **2**, 1808 (1969).
[14] C. Calandra and O. Bisi, Phys. Rev. B **31**, 8288 (1985).
[15] L. F. Mattheiss, Phys. Rev. B **43**, 1863 (1991); **43**, 12 549 (1991); **45**, 3252 (1992).